E-ISSN: 2664-7583 P-ISSN: 2664-7575 Impact Factor (RJIF): 8.12 IJOS 2025; 7(2): 285-294 © 2025 IJPA

www.physicsjournal.in

Received: 26-09-2025 Accepted: 29-10-2025

Tareq A Al Attabi

1. University of Sumer, Rifai 66001, Iraq 2. Department of Physics, College of Sciences, University of Thi-Qar, Iraq

Salam Jasim Majeed

Department of Mathematics, College of computer science and Mathematics, University of Thi-Qar, Iraq

Muwaffaq Abdullah

Department of Physics, College of Sciences, University of Thi-Qar, Iraq

Corresponding Author: Tareq A Al Attabi

1. University of Sumer, Rifai 66001, Iraq 2. Department of Physics, College of Sciences, University of Thi-Qar, Iraq

Analytical study of the behavior of semiconductor lasers under optoelectronic feedback

Tareq A Al Attabi, Salam Jasim Majeed and Muwaffaq Abdullah

DOI: https://doi.org/10.33545/26647575.2025.v7.i2d.204

Abstrac

Studying the dynamics of semiconductor lasers (SLs) is crucial for advancing a wide range of optical technologies. SLs exhibit rich dynamical phenomena, and these behaviors can be harnessed for many novel applications. The chaotic behavior dynamics of SLs with optoelectronic feedback (OEFB) have been studied theoretically. After a series of mathematical operations, they were converted into dimensionless equations. Further, after testing these equations analytically. The results show the SL model always has one internal equilibrium point Σ° , if the parameter values (x, k) take positive values and until after adding the feed-delayed effect to the above model. While it was observed that the point loses its stability when the value of the feed delay takes a positive $(\tau_d > 0)$, where the solution paths of x, u, and u take a periodic form near Σ° . Further, the generalized system may undergo a Hopf bifurcation about Σ° .

Keywords: BSLs, OEFB, dynamics, equilibrium points, Hopf.

Introduction

Studying the behavior and dynamics of a laser system through rate equations is crucial for several reasons to understand laser dynamics. Rate equations help in understanding how populations of various energy levels change over time under the influence of pumping and laser radiation. This understanding is essential for optimizing laser performance and stability. By solving rate equations for laser behavior, researchers can predict the transient and steady-state behavior of lasers. This includes phenomena like threshold behavior, relaxation oscillations, and the evolution of photon number in the laser cavity [1, 2]. Rate equations provide insights into the minimum pumping rate required to achieve population inversion, which is necessary for laser action. This helps in designing lasers that are more efficient and effective for various applications [3]. The equations can be used to determine the optimal output coupling for maximizing the output power of a laser. This is particularly important for applications requiring high-intensity laser beams [4].

Studying the stability and bifurcation of a laser system helps us to understand stability and helps predict how a laser will respond to changes in parameters such as pump power, cavity losses, and external feedback. This is essential for designing stable laser systems that perform reliably under various conditions. By analyzing bifurcations, researchers can identify critical points where the laser's behavior changes dramatically ^[5, 6]. This knowledge allows for the optimization of laser parameters to achieve desired performance, such as higher output power or specific wavelength emission. Stability analysis helps identify and avoid undesirable behaviors like chaos or mode hopping, which can degrade laser performance ^[7, 8]. By understanding these dynamics, engineers can design control strategies to mitigate such effects. Rate equations provide a framework for developing control mechanisms to stabilize lasers and maintain their operation within desired regimes. This is particularly important for applications requiring precise and stable laser output ^[9].

Theoretical model

From the physical model of two-level atoms in SLs, the differential equation for the carrier density N, which is equivalent to the population inversion in common lasers.

The interactions between photon density S and carrier density N can be articulated by the conventional single-mode SL rate equations, suitably adjusted to incorporate the ac-coupled feedback loop [10]:

$$\dot{S} = \left[g(N - N_t) - \gamma_{\circ}\right] S + \frac{\gamma g}{u_{\circ}(N - N_t)}$$

$$N' = \{I_\circ + f(I)\}/eV - \gamma_c N - g(N - Nt)S$$
 (1)

 $\dot{I} = \gamma_f I + K \dot{S}$ where g the differential gain, N(t) the carrier density at transparency, Nth the carrier density at threshold, and the analysis of the fundamental dynamics of instability and chaos in nonlinear systems could be conducted solely with deterministic terms, without statistical noise. Noise is fundamentally regarded as a distinct phenomenon from chaotic oscillations, provided it remains minimal.

where I is the high-pass filtered feedback current (before the nonlinear amplifier), f (I) \equiv AI/(1+s'I) is the feedback amplifier function, Io is the bias current, e the electron charge, V is the active layer volume, γ 0 and γ c are the photon damping and population relaxation rate, respectively, γ f is the cutoff frequency and k is a coefficient proportional to the photo detector responsivity.

In contrast to optical feedback, optoelectronic feedback is dependable and resilient due to the system's insensitivity to optical phase fluctuations. Consequently, the phase dynamics of the optical field can be disregarded. A comprehensive physical model of the system must incorporate a series of low-pass frequency filters resulting from the photodiode's limited bandwidth, the electrical connections to the laser, parasitic capacitances, and other adverse electronic effects [11]. For numerical and analytical purposes, it is useful to rewrite Eqs. (1) in dimensionless form. To this end, we introduce the new variables: $x = (g/\gamma c) S$, $y = g/\gamma o$ (N-Nt), $w = (g/k\gamma c) I-x$, and the time scale $t` = \gamma ot$. The rate equations then become as following:

The first rate equation is:

$$\dot{x} = x(y-1) + yy,$$

$$\dot{y} = y \left(\delta_{\circ} - y + \alpha \frac{w+x}{1+\delta(w+x)} - xy \right),$$

$$\dot{w} = -\epsilon (w+x).$$
(2)

where δ_{\circ} is the bias current and \in is the feedback strength. These are rate equations of SL in dimensionless form in order to compute and for numerical and analytical purposes.

These equations representing the nonlinear dynamical system which produced HC in SL with OEFB. The first equation represents the photon density or the intensity for output laser ray, the second equation represents the population inversion, while the third equation represents the feedback which is necessary to produce chaos this feedback consist from the intensity of laser output and the current bias.

Interior Equilibrium of the Model (2)

In this section, we investigate the existence of the non-boundary equilibrium point of the system (2). To do that the following equations must be solve:

$$x(y-1) + xy = 0,$$

$$x\left(\delta_{\circ} - y + \alpha \frac{w+x}{1+\delta(w+x)} - xy\right) = 0,$$

$$-\epsilon (w+x) = 0.$$

For solving the above system when $r \neq 0$, $\epsilon \neq 0$, and $\alpha \neq 0$, one can have

$$x(y-1) + xy = 0,$$

$$\delta_{\circ} - y(1+x) = 0,$$

$$w + x = 0.$$

From first equation, we have

$$y^{\circ} = \frac{x^{\circ}}{x^{\circ} + x}.$$

Apply this in second equation gives

$$x^{\circ 2} + (1 - \delta_{\circ})x^{\circ} - \delta_{\circ}x = 0.$$

Hence can have

$$x^{\circ} = \frac{-\left(1-\delta_{\circ}\right) + \sqrt{(1-\delta_{\circ})^2 + 4\delta_{\circ}\tau}}{2} > 0.$$

Further third equation gain that

$$w^{\circ} = -x^{\circ}$$
.

Therefore, we can say the system has the interior equilibrium point $\Sigma^{\circ} = (x^{\circ}, y^{\circ}, -x^{\circ})$.

Stability Analysis of the Equilibrium Σ° of Model (2)

The main approach in this section is the analysis of nonlinear dynamical system (2) near the point Σ^* . The Jacobian linearization technique is used to find the local model that is linear in the state variables x and y.

System (2) at any point (x, y, w) has the next Jacobian matrix

$$M(x,y,w) = \begin{pmatrix} \frac{y-1}{\pi\alpha} & x+y & 0\\ \frac{y}{(1+\delta(x+w))^2} - yy & -y(1+x) & \frac{y}{(1+\delta(x+w))^2} \\ -\epsilon & 0 & -\epsilon \end{pmatrix}$$

This matrix, when $(x, y, w) = (x^{\circ}, y^{\circ}, -x^{\circ})$, reduced to

$$M^{\circ} = M(\Sigma^{\circ}) = \begin{pmatrix} y^{\circ} - 1 & x^{\circ} + x & 0 \\ x\alpha - xy^{\circ} & -x(1 + x^{\circ}) & x\alpha \\ -\epsilon & 0 & -\epsilon \end{pmatrix}.$$
(3)

The characteristic equation of M° is given by

$$|M^{\circ} - \lambda I| = 0,$$

or

$$\begin{vmatrix} (y^{\circ} - 1) - \lambda & x^{\circ} + \gamma & 0 \\ x\alpha - xy^{\circ} & -x(1 + x^{\circ}) - \lambda & x\alpha \\ -\epsilon & 0 & -\epsilon - \lambda \end{vmatrix} = 0.$$

The last equation gives

International Journal of Physics and Applications

$$\left(\left(y^{\circ} - 1 \right) - \lambda \right) \begin{vmatrix} - v(1 + x^{\circ}) - \lambda & v\alpha \\ 0 & - \epsilon - \lambda \end{vmatrix} - \left(x^{\circ} + \gamma \right) \begin{vmatrix} v\alpha - vy^{\circ} & v\alpha \\ -\epsilon & -\epsilon - \lambda \end{vmatrix} = 0,$$

which mean that

$$\left((y^{\circ}-1)-\lambda \right) (v(1+x^{\circ})+\lambda) (\in +\lambda) - (x^{\circ}+\gamma) [(v\alpha-vy^{\circ})(-\in -\lambda)+\varepsilon v\alpha] = 0,$$

The above equation can be written in the next polynomial form

$$\lambda^3 + a\lambda^2 + b\lambda + c = 0, (4)$$

where,

$$a = \in +r(1+x^{\circ}) - (y^{\circ} - 1),$$

$$b = \in r(1+x^{\circ}) - (\in +r(1+x^{\circ}))(y^{\circ} - 1) - (x^{\circ} + r)(r \propto -ry^{\circ}),$$

$$c = \in ry^{\circ}(x^{\circ} + r) - \in r(1+x^{\circ})(y^{\circ} - 1).$$

Therefore, matrix M° has three eigenvalues represented by the roots of Eq.(7), if the next conditions hold

$$0 < y^{\circ} < 1, \tag{5}$$

$$\Delta = ab - c > 0 \tag{6}$$

Clearly condition (5) gain \boldsymbol{a} and \boldsymbol{c} are positive. So in present of conditions (8) and (9), all conditions of Routh-Hurwitz criterion [8] are obtained. Hence, we have the following theorem.

Theorem (1): The point Σ° is locally asymptotically stably of the system of equations (2) when the above requirements (5) and (5) are met.

Delay model of system (2)

In theoretical physics, delay time is often used to describe the dynamic behavior of systems. Delay time helps in capturing the transient response of physical systems, allowing a more accurate representation of how systems evolve over time. In the presence of a time delay, the model can become unstable and show more intricate dynamic behaviors, such as Hopf bifurcation and saddle-node behavior. Specially, the features of periodic solutions resulting from the Hopf bifurcation hold great significance [12]. In actuality, temporal delays occur in a wide range of physical processes, including feedback systems, signal transmission, energy conversion, biological systems, chemical reactions, economic models, and more. Modeling real-world processes is helpful because many real-world processes, such as signal transmission and feedback loops, inherently involve delays. Incorporating delay time into models ensures these processes are accurately represented, [13, ^{14]}. Stability analysis with delay times is crucial for analyzing the stability of dynamic systems. Understanding how delays impact system behavior can help prevent oscillations or instability. In control systems or control theory, delay times are factored into the design of controllers to ensure that systems respond optimally, even with inherent delays [15]. Now model (2) is generalized to assume the following form using the discrete feed delay τ_d .

$$\dot{x} = x(y-1) + yy,$$

$$\dot{y} = y\left(\delta_{a} - y + \alpha \frac{w+x}{1+\delta(w+x)} - xy\right),$$

$$\dot{w} = -\epsilon \left(w + x(t - \tau_{d})\right).$$
(7)

Where τ_d is the time delay. It is well established that the location and number of equilibrium points remain constant despite time delay. Therefore system (7) still has the interior steady state solution Σ° .

Stability Analysis of the Equilibrium Σ° of Laser Bulk Model (7)

In the event of a time delay, the stability of model (7) may be effected. So, in this section, we examine the stability Σ° of generalized model (7). Due the presence of time delay τ_d system (7) has a generalized variational matrix that is as follows:

$$= \begin{pmatrix} y-1 & x+\pi & 0\\ \frac{\pi\alpha}{\left(1+\delta(x+w)\right)^2} - \pi y & -\pi(1+x) & \frac{\pi\alpha}{\left(1+\delta(x+w)\right)^2} \\ -\epsilon e^{-\lambda \tau_d} & 0 & -\epsilon \end{pmatrix}$$

For simplicity GM matrix at Σ° may be written as

$$GM^0 = \begin{pmatrix} A^0 & B^0 & 0 \\ C^0 & D^0 & E^0 \\ -\epsilon e^{-\lambda \tau_d} & 0 & -\epsilon \end{pmatrix},$$

where,
$$A^0 = y^0 - 1$$
, $B^0 = x^0 + y$, $C^0 = x(\alpha - y^0)$, $D^0 = -x(1 + x^0)$ and $E^0 = x\alpha$.

Therefore, the system (7) at Σ° has the next characteristic equation

$$\begin{vmatrix} A^0 - \lambda & B^0 & 0 \\ C^0 & D^0 - \lambda & E^0 \\ -\epsilon e^{-\lambda \tau_d} & 0 & -\epsilon - \lambda \end{vmatrix} = 0,$$

it is equivalent to

$$\lambda^3 + \bar{a}\lambda^2 + \bar{b}\lambda + \bar{c} + \bar{d}e^{-\lambda\tau_d} = 0, \tag{8}$$

where
$$\bar{a} = \epsilon - (A^0 + D^0)$$
, $\bar{b} = A^0 D^0 - (\epsilon A^0 + \epsilon D^0 + B^0 C^0)$, $\bar{c} = \epsilon (A^0 D^0 - B^0 C^0)$, $\bar{d} = \epsilon B^0 E^0$.

First, for $\tau_d = 0$, GM^0 and Eq. (8) reduce to M^0 and Eq. (3) at respectively. Then with the help of theorem (2), still we have Σ° as asymptotically stable point of system (7).

Now, when τ_d has positive value, Eq. (8) may have roots include positive real parts. In this case Eq. (5) must has roots

cross the imaginary axis, i.e. it has a pair of pure imaginary roots.

For check this pair of roots, represented by $\lambda = \pm i\sigma$, $(\sigma > 0)$, exist or not.

If this two values of λ exist, then they must satisfy Eq.(8). Through substituting $\lambda = \sigma i$ in Eq.(8), we derive that

$$-\sigma^{3}i - \bar{a}\sigma^{2} + \bar{b}\sigma i + \bar{c} + \bar{d}(\cos(\sigma \tau_{d}) - i\sin(\sigma \tau_{d})) = 0.$$

This equation has the next real and imaginary part:

$$\bar{d}\cos(\sigma\tau_d) = \bar{a}\sigma^2 - \bar{c},$$

$$\bar{d}\sin(\sigma\tau_d) = \bar{b}\sigma - \sigma^3.$$
(9)

The last equation gives

$$\cos(\sigma \tau_d) = (\bar{a}\sigma^2 - \bar{c})/\bar{d},$$

$$\sin(\sigma \tau_d) = (\bar{b}\sigma - \sigma^3)/\bar{d}.$$

After squaring $(9)_1$ and $(9)_2$, we may summing the resulting equations to obtain

$$\sigma^6 + \bar{h}_1 \sigma^4 + \bar{h}_2 \sigma^2 + \bar{h}_3 = 0, \tag{10}$$

where

$$ar{h}_1=ar{a}^2-2ar{b}$$
 , $ar{h}_2=ar{b}^2-2ar{a}$ $ar{c}$, and $ar{h}_3=ar{c}^2 ar{d}^2$.

Eq.(10) brings us to the subsequent equation after substituting each σ squared with $\overline{\sigma}$ (i.e. $\overline{\sigma} = \sigma^2$).

$$\bar{\sigma}^3 + \bar{h}_1 \bar{\sigma}^2 + \bar{h}_2 \bar{\sigma} + \bar{h}_3 = 0. \tag{11}$$

Accordance to Descartes' rule of signs, in the event that $h_1 > 0$ and $h_3 < 0$ are fulfilled, there is a unique positive root $\overline{\sigma}$ satisfying Eq. (11). Consequently, $\mp \sigma i$ represents two imaginary roots of Eq. (8).

Therefore, for different values of τ_d , system (7) may establish hopf bifurcation near Σ° . Let $\tau_0 = \min\{\tau_d\}$ at which a hopf bifurcation appears. In order to establish that, for $\tau_d = \tau_0$, we need to prove the next condition, denoted the transversality condition, is holds

$$sing \left\{ \frac{dRe\lambda(\tau_d)}{d\tau_d} \right\} > 0. \tag{12}$$

To achieve that, assume the root of Equation (8) fulfilling $\rho(\tau_0) = 0$, is $\lambda(\tau_d) = \rho(\tau_d) + i\sigma(\tau_d)$, where $\sigma(\tau_0) = \sigma_0$. Since λ is a function of τ_d , therefore, the differentiation of Equation (8) with regards to τ_d , can be expressed as follows:

$$\left[3\lambda^2 + 2\bar{a}\lambda + \bar{b} - \bar{d}\tau_d e^{-\lambda\tau_d}\right] \frac{d\lambda}{d\tau_d} - \bar{d}\lambda e^{-\lambda\tau_d} = 0,$$

and

$$\left(\frac{d\lambda}{d\tau_d}\right)^{-1} = \frac{3\lambda^2 + 2\bar{a}\lambda + \bar{b}}{\bar{d}\lambda} e^{\lambda\tau_d} - \frac{\tau_d}{\lambda}.$$
 (13)

With $(\tau_d = \tau_0, \lambda = i\sigma_0)$, one can have

$$3\lambda^2 + 2\bar{a}\lambda + \bar{b} = (\bar{b} - 3\sigma_0^2) + 2i\bar{a}\sigma_0,$$

$$(3\lambda^2 + 2\bar{a}\lambda + \bar{b})e^{\lambda\tau_d} = [(\bar{b} - 3\sigma_0^2) + 2i\bar{a}\sigma_0][\cos\sigma_0\tau_0 + i\sin\sigma_0\tau_0]$$

$$= \left[\left(\overline{b} - 3{\sigma_0}^2 \right) + 2i\overline{a}{\sigma_0} \right] \left[\frac{\overline{a}{\sigma_0}^2 - \overline{c}}{\overline{d}} + i \frac{\left(\overline{b}{\sigma_0} - {\sigma_0}^3 \right)}{\overline{d}} \right]$$

$$= \left[\left(\overline{b} - 3\sigma_0^2 \right) \frac{\overline{a}{\sigma_0}^2 - \overline{c}}{\overline{d}} - 2\overline{a}\sigma_0 \frac{\left(\overline{b}\sigma_0 - \sigma_0^3 \right)}{\overline{d}} \right]$$

$$+i\left[\left(\bar{b}-3{\sigma_0}^2\right)\frac{\left(\bar{b}{\sigma_0}-{\sigma_0}^3\right)}{\bar{d}}+2\bar{a}{\sigma_0}\frac{\bar{a}{\sigma_0}^2-\bar{c}}{\bar{d}}\right]$$

and

$$\bar{d}\lambda = i\bar{d}\sigma_0$$
,

further

$$\frac{\tau_d}{\lambda} = -i\frac{\tau_0}{\sigma_0}.$$

Then we have

$$Re\left[\frac{d\lambda}{d\tau_d}\right]_{\tau_d=\tau_0}^{-1}=Re\left[\frac{3\lambda^2+2\bar{a}\lambda+\bar{b}}{\bar{d}\lambda}e^{\lambda\tau_d}-\frac{\tau_d}{\lambda}\right]_{\lambda=i\sigma_0}$$

$$=Re\left[\frac{3\lambda^2+2\bar{a}\lambda+\bar{b}}{\bar{d}\lambda}e^{\lambda\tau_d}\right]_{\lambda=i\sigma_0}$$

$$=\frac{1}{\bar{d}\sigma_0}\left[\left(\bar{b}-3{\sigma_0}^2\right)\frac{\left(\bar{b}\sigma_0-{\sigma_0}^3\right)}{\bar{d}}+2\bar{a}{\sigma_0}\frac{\bar{a}{\sigma_0}^2-\bar{c}}{\bar{d}}\right]$$

$$=\frac{1}{\bar{d}^2}\left[\left(\bar{b}-3{\sigma_0}^2\right)\left(\bar{b}-{\sigma_0}^2\right)+2\bar{a}(\bar{a}{\sigma_0}^2-\bar{c})\right]$$

$$= \frac{1}{\bar{d}^2} \left[3\sigma_0^4 + 2(\bar{a}^2 - 2\bar{b})\sigma_0^2 + \bar{b}^2 - 2\bar{a}\bar{c} \right]$$

$$= \frac{1}{\bar{d}^2} \left[3{\sigma_0}^4 + 2\bar{h}_1{\sigma_0}^2 + \bar{h}_2 \right]$$

$$=\frac{1}{\bar{d}^2}\bar{h}(\sigma_0^2),$$

Where,
$$\bar{h}(\sigma_0^2) = 3\sigma_0^4 + 2\bar{h}_1\sigma_0^2 + \bar{h}_2$$
.

Let $\varkappa = \sigma_0^2 > 0$, then one can show that from complex analysis

$$sing \left[\frac{d(\operatorname{Re} \lambda(\tau_d))}{d\tau_d} \right]_{\tau_d = \tau_0}^{-1} = sing \operatorname{Re} \left[\frac{d\lambda(\tau_d)}{d\tau_d} \right]_{\tau_d = \tau_0}^{-1} = sing \left[\overline{h}(\varkappa) \right].$$

Clear we have $\bar{h}'(\varkappa) = 6\varkappa + 2\bar{h}_1 > 0$. So that in $[0, \infty]$, $\bar{h}(\varkappa)$ is monotonously increases.

Furthermore, with the condition

$$\bar{b}^2 > 2\bar{a} \, \bar{c}_{i} \, (14)$$

On can get $\bar{h}(0) > 0$, and $\bar{h}(\varkappa) > 0$ for $\sigma > 0$.

Consequently, the transversal condition (13) is satisfy if condition (14) is met.

Theorem (2): Assume that the condition (14) holds, then when $\tau_d \in [0; \tau_0)$ all roots of equation (8) have negative real parts, and when $\tau_d = \tau_0$ equation (8) has a pair of purely imaginary roots $\pm i\sigma$ while all other roots have negative real parts.

Numerical Simulations

Numerical simulations are offered in this section to back up our analytical findings. These simulations also reveal the system's fascinating, complicated behavior. For a hypothetical collection of data, numerical simulations are run using the Matlab software.

Table 1: Parameters used in our numerical simulation of laser bulk, [7, 9]

Parameters	Value
x	0.01
δ_{\circ}	1.0058011
α	1.007
δ	0.2
E	5e-4

First, in order to investigate the impact of varying parameter values (such as a and) on the dynamical behavior of the model of laser bulk (2), the following results are observed. Time series analysis is applied to the dynamical behavior of the laser bulk model physically, where it typically represents the evolution of measurable quantities like the number of photons of the emitted light, charge carriers, and phase of the bias current. These variables evolve over time according to nonlinear differential equations, often exhibiting complex behaviors such as relaxation oscillations, period doubling, and chaos.

Figure (1), with the data set in table (1), shows that the trajectories of the laser bulk model (2) converge to interior equilibrium $\Sigma^{\circ} = (0.1032 , 0.9117, -0.1032)$. Further, the time series of the behaviors of **x**, **y** and **w** show that the conditions (5) and (6) hold where, $y^{\circ} = 0.9117 < 1$, and $\Delta = 104e^{-8} > 0$. Moreover, the numerical solution gives that the eigenvalues of the Jacobian matrix GM^{0} are $\lambda_{1} = -0.0075$, $\lambda_{2} = -0.0003 + 0.0002i$ and $\lambda_{3} = -0.0003 - 0.0002i$. Then from theorem (1) the dynamic of model (2) is locally asymptotically stabile near

 Σ . The stable behavior of both y and w is due to the statistical change in the number of electrons in the beam, while the variable behavior of x is due to the initial turn-on processes that appear during the first pulse and then tend towards stability. Studying the turn-on behavior in lasers is essential for both fundamental understanding and practical applications in photonics, optoelectronics, and high-speed communication systems. The turn-on delay time between applying current and the onset of lasing is critical in pulsed and modulated laser systems. It affects data transmission rates, especially in optical communication where turn-on behavior precision matters.

On the other hand, to show the effect of time delay of feed (τ_d) on the switches, the stability of laser bulk model (2). The numerical solutions of the laser bulk model (7) for parameter values as given in table (1) with $\tau_d > 0$ are plotted in the next figures. In Fig.(2) and Fig. (3), with $\tau_{d=}70$ and other parameters as given in table (1), the time series and phase portrait of the model are plotted, respectively. With these parameter values equation (10) takes the form $\sigma^6 + 0.00814\sigma^4 + 0.00753e^{-3}\sigma^2 - 0.00137e^{-10} = 0$,

hence, we have the unique positive root $\sigma=0.00182 e^{-4}$. Therefore Eq. (8) has the two pure imaginary roots $\sigma=\mp 0.00182 e^{-4}$. Furthermore, the transversality condition (12) holds where the condition (14) holds as $\bar{b}^2=8.39160849 e^{-7}>2\bar{a}\;\bar{c}=8.65053994 e^{-8}$

Therefore, due to theorem (2) system (7) undergoes a Hopf-bifurcation, and a periodic solution occurs around Σ^* as depicted in Figs. (2) and (3).

Also, the effect of τ_d with increasing the value of bias current δ_{\bullet} the dynamic of model (2) broches to a limit cycle oscillation near the interior equilibrium point Σ^{\bullet} as shown in Figs.(4), (5) and (6). The sharp peaks indicate the unique property of optoelectronic feedback that distinguishes it from other cases. The effect of the delay time on the overall behavior is also shown in the delay time of the first pulse in Fig. (6), where the delay time directly affects the timing of the first pulse and subsequent pulses. For example, in systems with sharp optoelectronic feedback peaks, the delay determines when the first pulse emerges and how the pulse train evolves.

Figures (7), (8), (9), and (10) exhibit a variety of behaviors, ranging from periodic to quasi-periodic, all the way to chaotic. This variation in behavior is primarily due to the delay time and its effect on the phase. The delayed time effect in laser dynamics, particularly in systems with optoelectronic feedback, plays a pivotal role in shaping the behavior of the laser output. Where the feedback loop introduces a temporal lag that can dramatically influence the laser's behavior. Induced oscillations and chaos delay can destabilize steady-state laser output, leading to periodic oscillations or even chaotic behavior. This is especially prominent in semiconductor lasers [16].

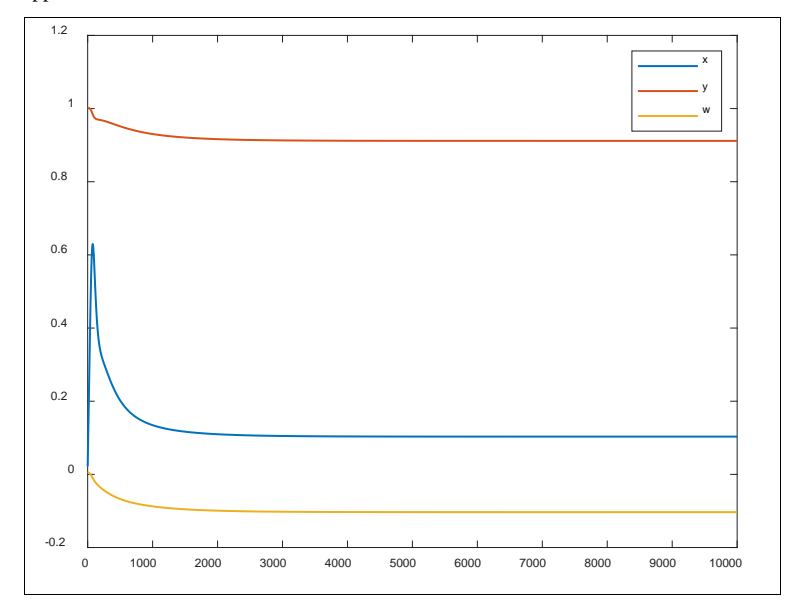


Fig 1: The time series for the laser bulk model (2) with for data in Table (1).

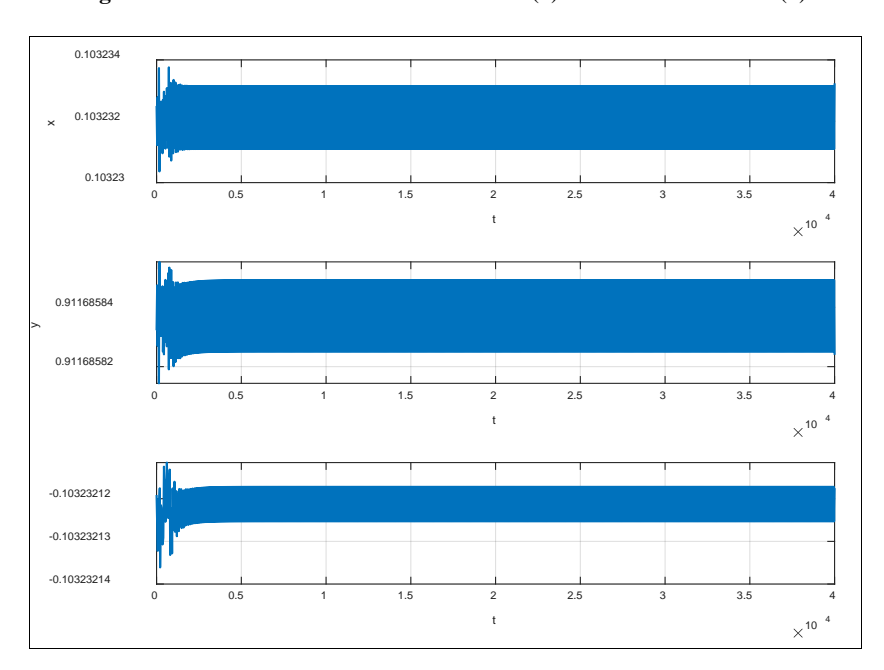


Fig 2: The time series for the laser bulk model (7) with data in Table 1 and $\tau_{d=}$ 70.

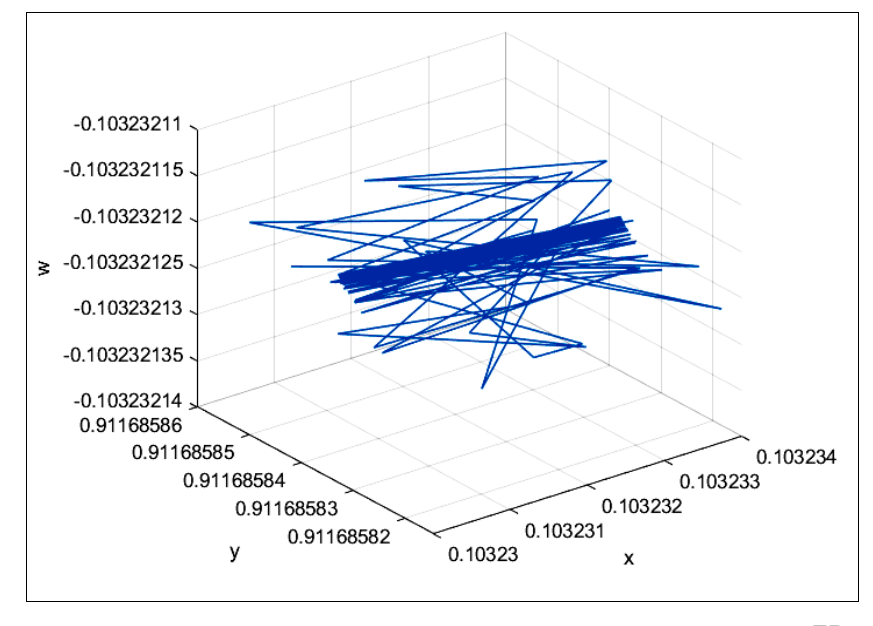


Fig 3: Phase portrait for the laser bulk model (7) with data in Table 1 and $\tau_d=70$.

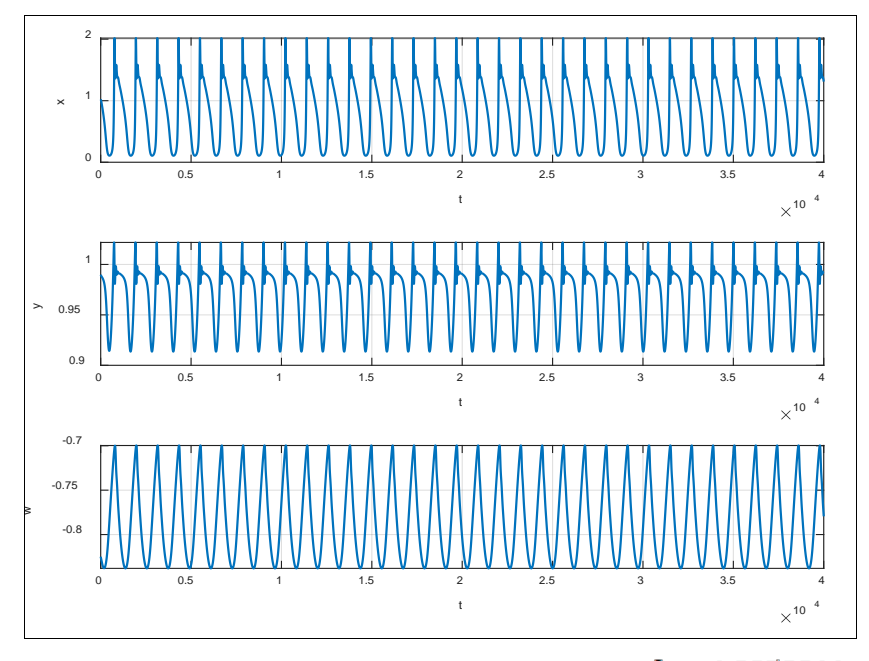


Fig 4: The time series for the laser bulk model (7) with data in Table 1 with $\delta_{\rm o}=1.8058011$ and $\tau_{d=}70$.

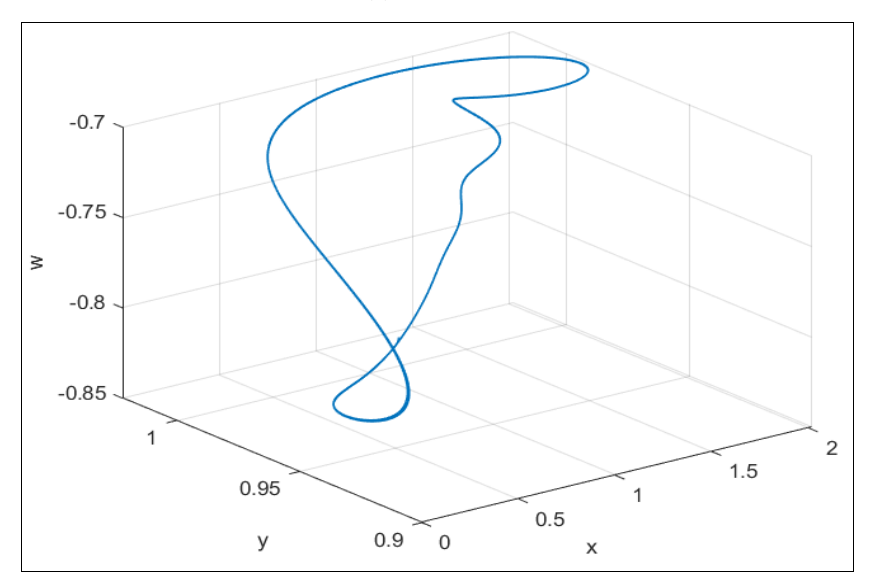


Fig 5: Phase portrait for the laser bulk model (7) with data in Table 1 with $\delta_{\text{a}}=1.8058011$ and $\tau_{d=}70$.

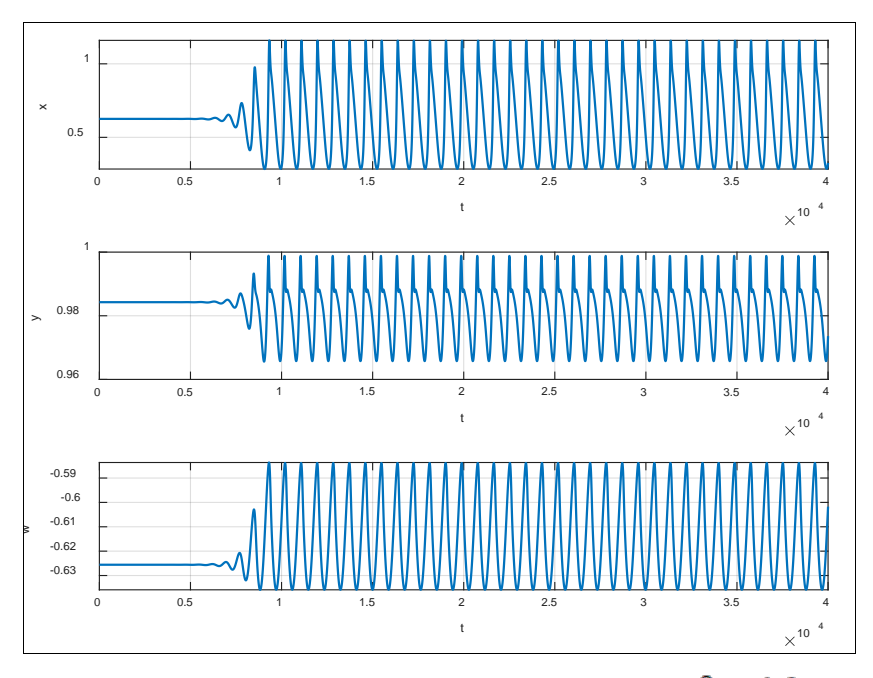


Fig 6: The time series for the laser bulk model (7) with data in Table 1 with $\delta_0 = 1.6$ and $\tau_{d=}70$.

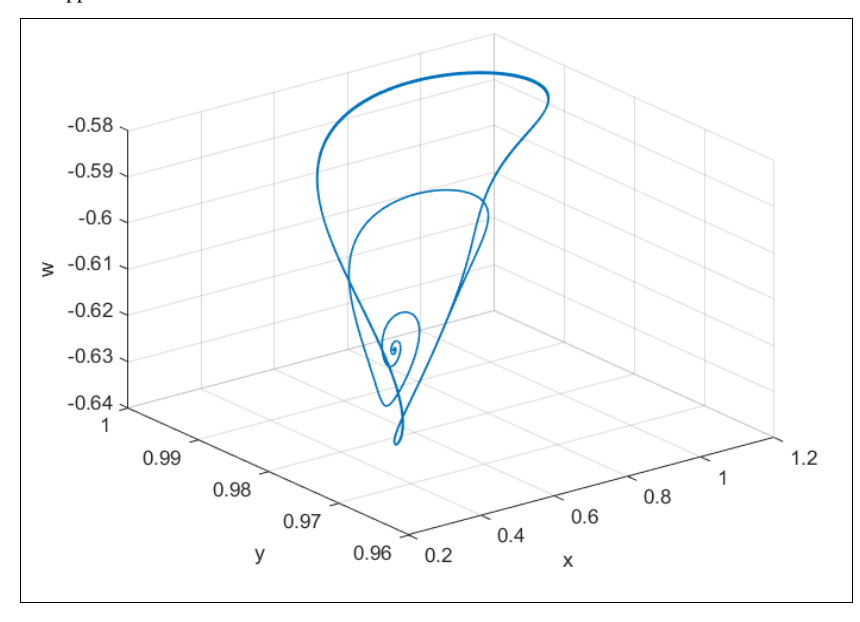


Fig 7: Phase portrait for the laser bulk model (7) with data in Table 1 with δ = 1.6 and $\tau_{d=}$ 70

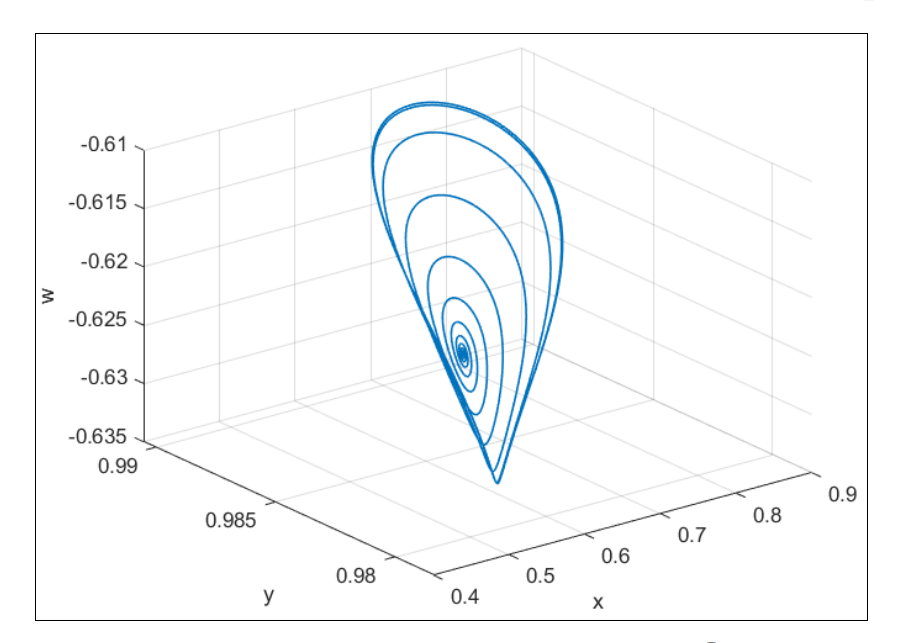


Fig 8: Phase portrait for the laser bulk model (7) with data in Table 1 with $\delta_{\rm m}=1.6$ and $\tau_{d=}30$.

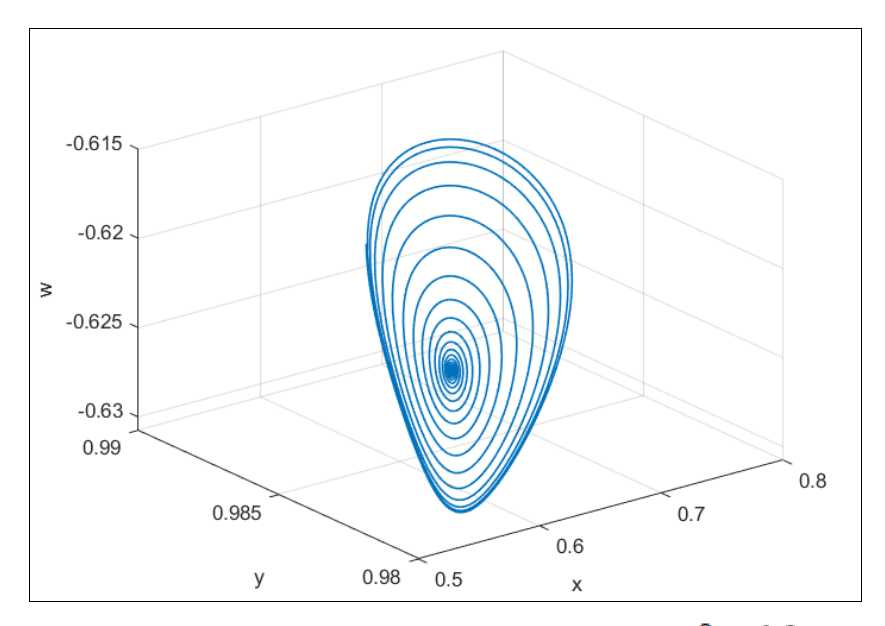


Fig 9: Phase portrait for the laser bulk model (7) with data in Table 1 with $\delta_\circ=1.6$ and $\tau_{d=}20$.

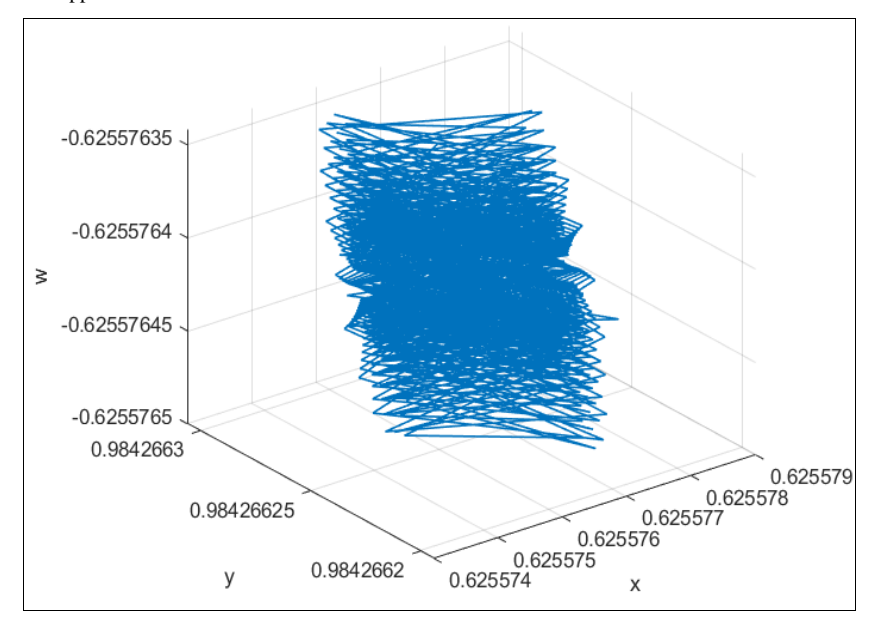


Fig 10: Phase portrait for the laser bulk model (7) with data in Table 1 with $\delta_0 = 1.6$ and $\tau_{d=}$ 15.

Conclusion

A theoretical study has been done on the chaotic behavior dynamics of SLs with OEFB. In this investigation, the following conclusions can be drawn. Mathematical model was proposed for the work of the SL system, which consists of three equations that were chosen from a mathematical SL model. Also, after a series of mathematical operations, these equations were converted into dimensionless equations. On the analytical side, the following was observed:

- The bulk laser model always has one internal equilibrium point Σ° , if the parameter values (\mathbf{v}, k) take positive values
- If the conditions $\alpha < u^* < 1, \Delta = ab c > 0$ are met, the dynamic system of the model is stable at the point Σ^* .
- After adding the feed delayed effect to the above model and obtaining a more general model, we note that the generalized model also still has one internal equilibrium point Σ[®].
- It was observed that the point loses its stability when the value of the feed delay take a positive $(\tau_d > 0)$, where the solution paths of x, u, and w take a periodic forms near Σ° . Further the generalized system may undergoes a Hopf- bifurcation about Σ° , Moreover, with changing the value of the feed delay, the system solutions may approach to a limit cycle around the point Σ° .

Acknowledgments. The authors thank Proof. Dr. Hussein B. AL-Husseini, Al-Ayen Iraqi University, Nassiriya, Iraq, for their cooperation in achieving these theoretical results. This work is supported by the Nassiriya Nanotechnology Research Laboratory (NNRL), Science College, University of Thi Qar, Iraq.

Compliance with ethical standards

Conflicts of interest. The authors declare that they have no conflict of interest.

Author contributions. All the authors contributed equally in this work.

Data Availability Statement. Data are analyzed and included in this manuscript. The detailed data could be shared with the corresponded author upon a reasonable request.

References

- 1. Al Attabi TA, Al Husseini HB. Equilibrium points, linear stability, and bifurcation analysis on the dynamics of a quantum dot light emitting diode system. Journal of Optical Communications. 2025;46(1):93-105.
- Mahdi AS, Al Husseini HB. Filtered optical feedback modes effect on quantum-dot laser behavior. Journal of Optics (India). 2024;53(3):1972-1983.
- 3. Kareem ZS, Al Husseini HB. Study of the dynamic properties of chaotic circuits in the presence of memristors. International Journal of Thin Film Science and Technology. 2024;13(2):153-168.
- 4. Mahdi AS, Al Husseini HB. Quantum dot laser dynamics and external filtered modes under the influence of double-filtered optical feedback. Physica Scripta. 2024;99(4):045108.
- 5. Ali HM, Al Husseini HB. Synchronization of chaotic network quantum dot light-emitting diodes under optical feedback. Journal of Optics (India). 2020;49(4):573-579.
- Rogister F, Locquet A, Pieroux D, Sciamanna M, Deparis O, Megret P, et al. Secure communication scheme using chaotic laser diodes subject to incoherent optical feedback and incoherent optical injection. Optics Letters. 2001;26:1486-1488.
- Saucedo Solorio JM, Sukow DW, Hicks DR, Gavrielides A. Bifurcations in a semiconductor laser subject to delayed incoherent feedback. Optics Communications. 2002;214:327-334.
- 8. May RM. Stability and complexity in model ecosystems. Princeton (NJ): Princeton University Press; 1973.
- 9. Sabharwal R. Introduction to System Dynamics. New Delhi: Educohack Press; 2025.
- Irhaif WK, Al Husseini HB. Stability analysis and bifurcation in external cavity quantum dot semiconductor laser. 2nd International Scientific Conference of Al-Ayen University (ISCAU-2020). IOP Conference Series: Materials Science and Engineering. 2020;928:072042. doi:10.1088/1757-899X/928/7/072042.

- 11. Al-Naimee K, Marino F, Ciszak M, Meucci R, Arecchi FT. Chaotic spiking and incomplete homoclinic scenarios in semiconductor lasers with optoelectronic feedback. New Journal of Physics. 2009;11:073022(1-11).
- 12. Buraimoh E, Ozkan G, Timilsina L, Chamarthi PK, Papari B, Edrington CS, *et al.* Overview of interface algorithms, interface signals, communication and delay in real-time co-simulation of distributed power systems. IEEE Access. 2023;11:103925-103955.
- 13. Nilsson J. Real-time control systems with delays. PhD Thesis. TFRT-1049. 1998.
- 14. Rionero S. Hopf bifurcations in dynamical systems. Ricerche di Matematica. 2019;68:811-840.
- Al-Naimee K, Marino F, Ciszak M, Abdalah SF, Meucci R, Arecchi FT. Excitability of periodic and chaotic attractors in semiconductor lasers with optoelectronic feedback. European Physical Journal D. 2010;58:187-180
- Abudali RH, Ajeel SK, Mousa SK, Al Husseini HB. Phase-coupled synchronization with optoelectronic feedback. In: 2022 International Congress on Human-Computer Interaction, Optimization and Robotic Applications (HORA). Ankara, Turkey: IEEE; 2022. doi:10.1109/HORA55278.2022.9799889.